Proc. Natl. Acad. Sci. USA
Vol. 91, pp. 1667–1671, March 1994
Biophysics

A collision gradient method to determine the immersion depth of nitroxides in lipid bilayers: Application to spin-labeled mutants of bacteriorhodopsin

CHRISTIAN ALTENBACH†, DUNCAN A. GREENHALGH‡§, H. GOBIND KHORANA‡, AND WAYNE L. HUBBELL†

†Jules Stein Eye Institute and Department of Chemistry and Biochemistry, University of California Los Angeles, CA 90024-7008; and ‡Departments of Biology and Chemistry, Massachusetts Institute of Technology, 77 Massachusetts Avenue, Cambridge, MA 02139

Contributed by H. Gobind Khorana, August 27, 1993

ABSTRACT **Ten mutants of bacteriorhodopsin, each containing a single cysteine residue regularly spaced along helix D and facing the lipid bilayer, were derivatized with a nitroxide spin label. Collision rates of the nitroxide with apolar oxygen increased with distance from the membrane/solution interface. Collision rates with polar metal ion complexes decreased over the same distance. Although the collision rates depend on steric constraints imposed by the local protein structure and on the depth in the membrane, the ratio of the collision rate of oxygen to those of a polar metal ion complex is independent of structural features of the protein. The logarithm of the ratio is a linear function of depth within the membrane. Calibration of this ratio parameter with spin-labeled phospholipids allows localization of the individual nitroxides, and hence the bacteriorhodopsin molecule, relative to the plane of the phosphate groups of the bilayer. The spacing between residues is consistent with the pitch of an α-helix. These results provide a general strategy for determining the immersion depth of nitroxides in bilayers.**

Site-directed spin labeling has become a powerful tool for determination of membrane protein structures and their disposition with respect to the bilayer (1–3). In previous studies, information on the region where transmembrane helices intersect with the membrane/solution interface has been obtained by analysis of a consecutive series of mutants that traverse the interface (1). If it were possible to determine the vertical distance of a spin-labeled side chain from the plane of the phosphates of the lipid headgroups, analysis of only one or two spin-labeled mutants would be sufficient to determine the position of a transmembrane domain relative to the membrane.

EPR methods for estimation of the depth of immersion of a nitroxide in the membrane have been reported (4–6). These methods are based upon the dipolar interactions of the nitroxide with paramagnetic reagents constrained to the aqueous phase and require knowledge of the spacial distribution of the paramagnetic reagents in solution. This distribution may be readily deduced for a pure bilayer with a nitroxide on a lipid chain, but not for a nitroxide attached to a protein in a bilayer. This is because the protein has an unknown excluded volume for the paramagnetic reagent in the aqueous phase.

In this report, we make use of site-directed spin labeling to introduce nitroxides along the entire length of helix D of bacteriorhodopsin (bR). The collision frequencies of the nitroxides with paramagnetic reagents are dependent upon position, and this effect is shown to provide an approach for localization of nitroxides in the membrane interior.

The publication costs of this article were defrayed in part by page charge payment. This article must therefore be hereby marked "*advertisement*" in accordance with 18 U.S.C. §1734 solely to indicate this fact.

MATERIALS AND METHODS

Egg yolk phosphatidylcholine (PC) and 1-palmitoyl-2-(*n*-doxylpalmitoyl) PC spin-labeled isomers with $n = 5, 7, 10, 12$, and 16 were obtained from Avanti Polar Lipids. Ethylenediamine-*N*,*N*′-diacetic acid (EDDA), nickel(II) acetylacetonate (NiAA), and $Ni(OH)_2$ were obtained from Aldrich. bR mutants were prepared, spin labeled, and reconstituted as described (7) except that egg PC (Avanti) was substituted for asolectin to avoid negative membrane surface charges (2). All mutants were characterized in terms of the rate of chromophore formation, the absorption maximum of the chromophore (λ_{max}), and proton-pumping activity (8).

The nickel(II)–EDDA complex (NiEDDA) was prepared as follows: equimolar amounts of $Ni(OH)_2$ (464 mg) and EDDA (881 mg) were mixed in 100 ml of 50% methanol in water. The mixture was stirred for 24 hr at room temperature and an additional 24 hr at 60°C. The resulting blue solution was filtered, and the solvent was evaporated to give 1.12 g of a blue powder. Mass spectroscopy showed 1 peak at 231 Da (molecular ion $[NiEDDA - 1H]^-$).

EPR spectra were recorded as described (7) on a Varian EPR spectrometer equipped with a loop gap resonator and a gas permeable TPX plastic sample capillary. Power saturation curves were measured as the vertical peak-to-peak amplitude (A) of the first derivative $M_i = 0$ line as a function of incident microwave power (P) in the range of 0.1 to 36 mW. The resulting data were fitted to the function

$$A = I \cdot P^{1/2} \cdot [1 + (2^{1/\varepsilon} - 1)P/P_{1/2}]^{-\varepsilon},$$

with I, $P_{1/2}$, and ε as adjustable parameters. This function describes the saturation parameter of a first derivative EPR signal of arbitrary homogeneity and was sufficient to describe all data accurately. I is a scaling factor, $P_{1/2}$ is the power where the first derivative amplitude is reduced to half of its unsaturated value, and ε is a measure of the homogeneity of saturation of the resonance line. For the homogeneous and inhomogeneous saturation limits, $\varepsilon = 1.5$ and $\varepsilon = 0.5$, respectively. Under nitrogen and at relatively low collision frequencies, ε was always very close to 1.5, indicating homogeneous saturation. The quantity $\Delta P_{1/2}$ is the difference in $P_{1/2}$ values in the presence and absence of relaxing agent. To correct for effective spin–spin relaxation time (T_2^*) effects in comparing saturation curves of spin labels with different line shape, $\Delta P_{1/2}$ is divided by the *p*–*p* linewidth, ΔH^* (9), and normalized by the same quantity for a diphenyldipicrylhydrazide standard sample to correct for variations in resonator

Abbreviations: bR, bacteriorhodopsin; PC, phosphatidylcholine; NiAA, nickel(II) acetylacetonate; EDDA, ethylenediamine-*N*,*N*′-diacetic acid; NiEDDA, nickel(II)–EDDA complex; DMPC, dimyristoyl PC; T_1, spin–lattice relaxation time; T_2, spin–spin relaxation time.

§Present address: Testa, Hurwitz and Thibeault, Patent Department, 53 State Street, Boston, MA 02109.

properties to generate the dimensionless quantity Π, which is proportional to the collision frequency (10).

THEORY

Small molecules in a membrane/water system are partitioned between the water and the fluid hydrophobic phase of the bilayer according to their polarity. Polar molecules preferentially partition into the aqueous phase, and nonpolar molecules preferentially partition into the membrane phase. The bilayer interior, however, is nonuniform, with gradients of fluidity (11, 12) and polarity (13) along the direction of the bilayer normal. Thus there are expected to be gradients in both concentration and diffusion coefficients of small molecules in equilibrium with the aqueous phase. The concentration gradient at equilibrium can be described by a distance-dependent standard chemical potential in the bilayer phase:

$$C_{i,\mathrm{m}}(x) = C_{i,\mathrm{w}}\, e^{\frac{\mu^{\circ}_{i,\mathrm{w}}}{RT}}\, e^{\frac{-\mu^{\circ}_{i,\mathrm{m}}(x)}{RT}}, \qquad [1]$$

where $C_{i,\mathrm{m}}(x)$ is the concentration of species i in the bilayer at a distance x from the interface, $C_{i,\mathrm{w}}$ is the uniform concentration of neutral species i in the aqueous phase, and $\mu^{\circ}_{i,\mathrm{m}}$ and $\mu^{\circ}_{i,\mathrm{w}}$ are the corresponding Henry's law standard state chemical potentials. Nitroxide sites located on the protein surface are expected to have a depth-dependent collision rate with a paramagnetic reagent in partition equilibrium due to the above gradient. The Heisenberg exchange rate, W_{ex}, with a reagent diffusing in the lipid phase is proportional to collision rate and can be expressed as (14)

$$W_{\mathrm{ex}} = 4\pi p g d D_{\mathrm{m}}(x) C_{\mathrm{m}}(x), \qquad [2]$$

where p is the exchange probability, g is a steric factor, d is the collision diameter, $D_{\mathrm{m}}(x)$ is the position-dependent relative diffusion coefficient, and $C_{\mathrm{m}}(x)$ is the position-dependent concentration given by Eq. 1. The exchange rate is thus related to the depth in the bilayer, x, but is a complex function of steric factors, diffusion constants, and concentrations at different depths. For two paramagnetic reagents with similar sizes, the *ratio* of the exchange rates with a given nitroxide is independent of steric factors and would depend on distance through the concentration gradient only. The interaction of fast-relaxing paramagnetic reagents such as O_2 and NiAA with nitroxides in fluid media is dominated by Heisenberg exchange and produces changes in the spin–lattice relaxation time (T_1) proportional to W_{ex} (15). The experimental quantity $\Delta P_{1/2}$ is related to the exchange rate according to

$$\Delta P_{1/2} \propto W_{\mathrm{ex}}/T^{*}_{2\mathrm{e}} \qquad [3]$$

where $T^{*}_{2\mathrm{e}}$ is the electron spin–spin relaxation time. From Eqs. 1–3, it follows that the logarithm of the ratio of saturation parameters (Φ),

$$\Phi = \ln\frac{\Delta P_{1/2}(1)}{\Delta P_{1/2}(2)} = -\frac{[\mu^{\circ}_1(x) - \mu^{\circ}_2(x)]}{RT} + \text{constant}, \qquad [4]$$

is directly related to the difference in standard state chemical potentials of the reagents at any depth, independent of viscosity or steric constraints imposed by the environment and also independent of the EPR lineshape, since T^{*}_{2} cancels out. If the standard chemical potentials have a simple monotonic depth dependence, then Φ for two similar-sized reagents of different partition properties will be a useful measure of depth.

RESULTS

A structural model of bR based on electron diffraction (16) and earlier EPR results (1) is shown in Fig. 1 with the positions of the cysteine mutants indicated. Each mutant refolded with kinetics similar to the wild-type bR (Table 1). The absorption maxima and proton-pumping activities of the refolded mutants were indistinguishable from wild-type bR (Table 1). The values were similar for the underivatized and spin-labeled samples, suggesting that the spin labels do not affect either the structure or function of the proteins. These results are not surprising, since all the mutant side chains were chosen to be on the outer surface of helix D.

The EPR spectra of the spin labeled mutants are shown in Fig. 2. The EPR lineshape of the nitroxide at position 103, located in an interhelical loop, is characteristic of restricted motion, suggesting significant tertiary interactions. The lineshapes at positions 105–117 show that in each case the mobility of the nitroxide is high with little restriction, consistent with the side chains being on the outer helical surface. The lineshapes at positions 120–129 indicate more restriction in motion, even though these residues are expected to lie on the outer helical surface. This is discussed below.

Fig. 3 shows $\Pi(O_2)$ and Π(NiAA) as a function of side chain position. The $\Pi(O_2)$ value, and hence collision frequency, *increases* with depth in the membrane. This result is consistent with earlier work in which the collision rate of O_2 was determined for a series of spin-labeled fatty acids with nitroxides at different positions along the chain (17–19). However, unlike the case for simple fatty acids, the profile of collision rates here is asymmetric about the center of the bilayer. NiAA is a neutral but polar complex that has a small but finite solubility in the membrane. As shown in Fig. 3, Π(NiAA) *decreases* with depth in the membrane and mirrors the asymmetry seen with $\Pi(O_2)$.

In contrast, the quantity Φ, the logarithm of the *ratio* of the $\Delta P_{1/2}$ values (equivalent to the ratio of Π values), increases linearly from position 103 to 117, then decreases linearly from 117 to 129. The solid lines in Fig. 3 are the best linear approximations to the data. The Π(NiAA) values are maximal

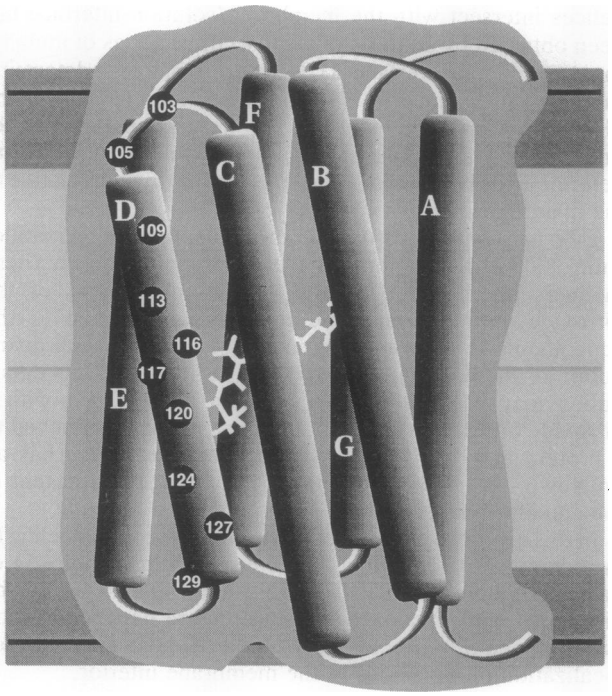

FIG. 1. bR model showing the positions of the residues investigated and the alignment of the protein with respect to the bilayer determined in this study (see text).

Table 1. Summary of the rates of chromophore formation, dark-adapted absorption maxima, and proton-pumping activities of the bR mutants before (−) and after (+) derivatization with the methanethiosulfonate spin label

Mutant	$t_{1/2}$ of chromophore formation*		λ_{max}, nm		Proton pumping†	
	−	+	−	+	−	+
Wild type	1.0	1.0	551	551	1.00	1.00
A103C	0.9	0.6	552	551	0.90	1.00
Q105C	1.0	0.8	551	550	0.80	1.00
L109C	0.9	0.8	552	550	0.85	1.05
G113C	1.1	0.7	550	551	0.95	1.00
G116C	1.1	0.9	550	550	1.00	1.10
I117C	1.8	1.1	550	548	0.95	1.05
G120C	2.1	0.3	551	552	1.05	0.95
V124C	1.5	0.4	551	552	1.10	1.10
L127C	1.6	0.6	551	550	1.00	1.00
K129C	1.1	0.3	553	552	0.85	0.85

*The $t_{1/2}$ values of chromophore formation were normalized to those of underivatized and derivatized bR. The $t_{1/2}$ of chromophore formation for wild-type bR was 1.6 min before and 3 min after the derivatization procedure.

†The initial rates of proton-pumping activity were normalized to wild-type bR (these values varied from 1 to 5 protons per bR per sec for wild type and were dependent on the batches of lipids and detergents used). Wild type was always assayed together with the mutants, providing an internal control for the proton-pumping assays.

at 105 and 129, indicating high collision rates with the polar NiAA, thus fixing these positions within the bilayer/aqueous interfacial domain. These results suggest that the position of the bR molecule is approximately as shown in Fig. 1. With this placement, the center of symmetry of Φ at 117 is located at the center of the bilayer. From this data alone, an approximate distance scale can be associated with the sequence axis in Fig. 3, since position 105 or 129 can be fixed at the interface

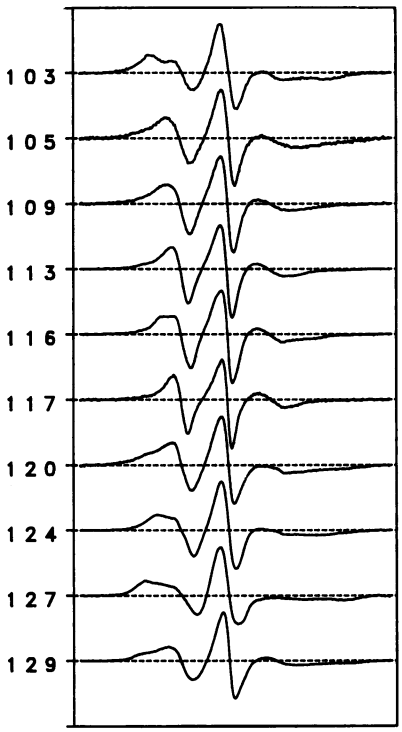

FIG. 2. Room temperature EPR spectra of spin-labeled bR mutants reconstituted in egg PC bilayers.

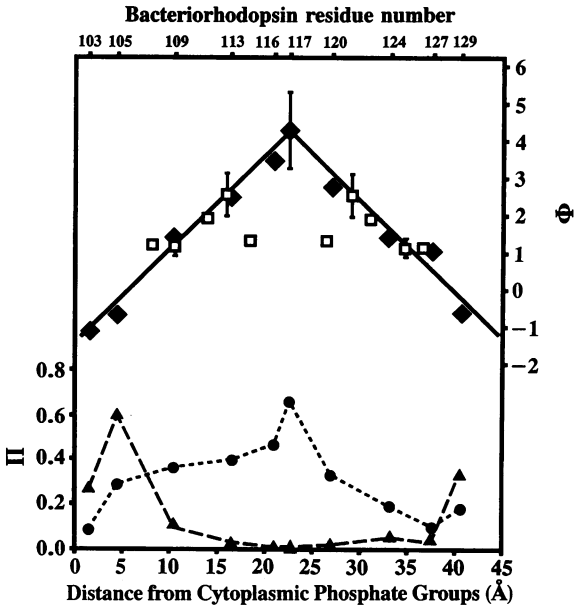

FIG. 3. $\Pi(O_2)$ (●), Π(NiAA) (▲), and the corresponding value of Φ (◆) for nitroxide side chains at the indicated positions. $\Pi(O_2)$ and Π(NiAA) were determined in equilibrium with air and in the presence of 20 mM NiAA, respectively. Also shown are Φ for the *n*-doxyl PC isomers under the same conditions (□). The distance scale was associated with the sequence axis using the *n*-doxyl PCs as described in the text.

and the incremental spacing of each nitroxide can be determined from the pitch of the D helix. A distance calibration based on the *n*-doxyl PCs can be employed to more precisely fix the location of the interface, since the location of these nitroxides relative to the plane of the phosphate groups is known. Fig. 3 also shows the results of identical measurements of *n*-doxyl PCs as a function of the distance of the nitroxide on the chain from the phosphate group (4, 10). Since the bilayers are symmetric and the *n*-doxyl PCs are uniformly distributed, the Φ values represent both halves of the bilayer and are plotted relative to both surfaces in Fig. 3. The Φ values for $n = 5$, 7, 10, and 12 yield a line with a slope very similar to that for the bR data. The Φ value for $n = 16$ does not fall on the line and is discussed below. Alignment of the bR data with that for the *n*-doxyl PCs links the individual residue numbers on bR with the known depths of the nitroxides on the phospholipids. This allows the determination of the protein side chain positions with respect to the phosphate group of the phospholipid. With this calibration of distance, the overall phosphate-to-phosphate membrane thickness in the vicinity of the protein is about 45 Å, which is consistent with the value from x-ray diffraction of 43 Å (20). The pitch of an α-helix is 1.5 Å per residue; therefore, the total distance from residues 105 to 129 is 37.5 Å, which is in good agreement with the distance of 37 Å determined from the plot. The alignment of bR shown in Fig. 1 is based on these results. Note that the center of the helical bundle coincides with the bilayer center.

If the relaxation mechanism for the nitroxide is dominated by collisions between the nitroxide and the paramagnetic reagent, then Π should reflect the solubility-diffusion product of the reagent in the bilayer interior. In turn, the solubilities of O_2 and NiAA in the bilayer are expected to depend on lipid composition and bilayer physical state. To investigate the effect of these variables, 7-doxyl PC was incorporated into dimyristoyl PC (DMPC) bilayers, and $\Pi(O_2)$, Π(NiAA), and Φ were analyzed as a function of temperature (Fig. 4). Unlike egg PC, DMPC has fully saturated fatty acid chains and exhibits a gel to liquid-crystalline phase transition at ≈23°C.

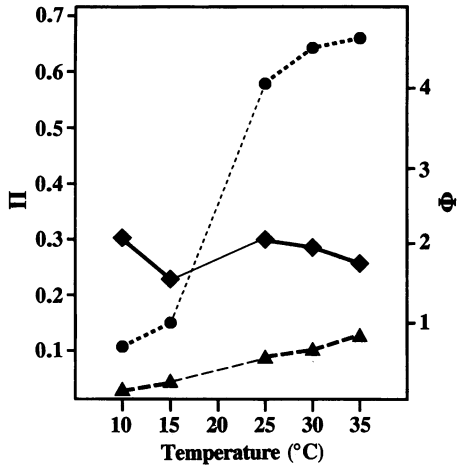

FIG. 4. Temperature dependence of $\Pi(O_2)$ (●) and Π(NiAA) (▲) and the corresponding value of Φ (◆) in DMPC for 7-doxyl PC. $\Pi(O_2)$ and Π(NiAA) were determined in equilibrium with air and in the presence of 20 mM NiAA, respectively.

As expected by a collisional mechanism, the Π values for both NiAA and O_2 are small below the phase transition and increase by a factor of ≈5 through the phase transition. The signals could not be saturated at the transition, so the Π and Φ values could not be determined between 15°C and 25°C. This has been observed previously for O_2 and may be due to anomalously high collision rates at the transition (21). The dotted lines connecting the 15°C and 25°C points in Fig. 4 are drawn only to guide the eye. Even though the Π values go through large changes with temperature, Φ changes less, by at most a factor of 1.4, even through the phase transition.

The Φ values for nitroxides at positions 120, 124, 127, and 129 were also determined using the neutral complex NiEDDA. The curve of Φ versus sequence (and distance) is approximately linear and parallel to that for Φ(NiAA). These results suggest that the linear relationship between Φ and distance is independent of the chemical identity of the metal ion complex.

DISCUSSION

The 10 bR mutants studied were selected to be regularly spaced along the lipid-exposed surface of the D helix, completely traversing the bilayer. The relatively high collision frequencies of the nitroxides at these positions with O_2 support this localization and confirm the published structural model in the monomeric state of bR (16). As noted above, the plots of both $\Pi(O_2)$ and Π(NiAA) versus sequence are asymmetric about the bilayer center. However, since the bilayer is symmetric, the asymmetry presumably arises from variations in the steric factor, g (Eq. 2), due to the local structural differences in the protein. The EPR lineshapes support this interpretation. The residues that have low Π values (120–129) are also those with restricted motions, indicating tertiary interaction of the nitroxide with other domains of the protein (Fig. 2).

The lineshapes and Π values contain information on both the local structure and distance from the membrane surface. Analysis of the spectra in terms of protein structure will be presented elsewhere. The objective of the present work is to extract the distance-dependent information. Assuming that steric constraints on collisions with the nitroxide side chains are similar for O_2 and NiAA, Φ should be independent of structure and dependent only upon distance (Eq. 4). This assumption is reasonable since the nitroxide spin labels are located on the surface of the protein and not buried in crevices that could discriminate between O_2 and NiAA based on size. Indeed, the linear, symmetric dependence of Φ on distance (Fig. 3) is consistent with this parameter being independent of local protein structure.

Since the positions of the nitroxides in the n-doxyl PCs relative to the plane of the phosphates of the bilayer can be calculated from x-ray and NMR data (4, 22), these molecules were used to provide an absolute distance calibration for the collision gradient. However, it is important to emphasize that the protein data alone provides an approximate distance calibration, and this is consistent with the n-doxyl PC data. The fact that the Φ parameters for a nitroxide on structures as different as a phospholipid and a protein surface are in agreement provides strong additional support for the structure independence of Φ (Fig. 3).

The simple dependence of Φ on distance from the interface makes it a useful quantity to determine the depth of immersion of nitroxides in bilayers, and Φ provides a tool for characterizing membrane proteins and the lipid bilayer using the site-directed spin-labeling technique. For practical applications, Φ should be calibrated with the n-doxyl PCs for the particular bilayer in use, since the individual gradients of O_2 and NiAA are expected to depend, to some extent, on the composition of the bilayer. In the present work, the calibration is for egg PC, since it is a lipid commonly employed in studies of membrane proteins. For approximate work, it may turn out that Φ is weakly dependent on lipid composition. This is suggested by the data in Fig. 4 for DMPC, where Φ for 7-doxyl PC is 2.0 at 25°C. A comparison of this value with that for 7-doxyl PC in egg PC at the same temperature (Φ = 1.2, Fig. 3) gives a depth differing by only a few angstroms. Further work is required to examine the generality of this result.

The Φ value for 16-doxyl PC deviates from the simple linear relationship shown in Fig. 3. Judging from previous work, this is not unexpected since polar moieties like the nitroxide attached near the terminal position of the chain result in a "bending back" of that position to the aqueous surface (15, 22). Thus n-doxyl PCs with nitroxides near the chain terminus should be used with caution. In future work focused on position-dependent phenomena in the bilayer, the series of bR mutants studied here will serve as a superior model system, since the nitroxides are rigidly fixed in position, and the small effect of the nitroxide is unlikely to cause vertical displacement of the large bR molecule.

The present method for depth determination requires two fast-relaxing paramagnetic species with finite but different solubilities in the bilayer. Molecular oxygen is an ideal choice for one. The metal ion complex used here, NiAA, does however have some undesirable properties. A solution of NiAA contains an equilibrium mixture of Ni^{2+}, $Ni(AA)_1^+$, $Ni(AA)_2^0$, and $Ni(AA)_3^-$ (23). At neutral pH, the uncharged species dominates, whereas at low (high) pH the equilibrium is shifted toward the positive (negative) species. Although the neutral species always dominates in the low dielectric interior of the bilayer, the presence of charged species will complicate analysis if the pH is either acidic or basic or if an electrostatic surface potential is present. This is not a problem in the present work since the lipid bears no charge, and the surface potential from bR is small in the relatively high ionic strength employed. This effect, however, restricts the use of NiAA. A promising candidate to overcome these problems is NiEDDA, a neutral, very small (M_r = 232) water-soluble complex that is stable down to low pH (only 1% free Ni^{2+} at pH 4). The partitioning into the membrane is less than that for NiAA, but this can be compensated for by using higher bulk concentrations. With 200 mM NiEDDA, the dependence of Φ on position is parallel to the results obtained with NiAA as shown in Fig. 3. Offset from the Φ(NiAA) curve depends on bulk concentration and relative partitioning into the membrane. Since this complex differs in size and

hydrophobicity from NiAA, the parallel lines indicate the absence of specific interactions and the independence of the method on choice of metal complex.

The mechanism of the enhanced relaxation of the nitroxides by O_2 and the metal ion complexes has been assumed to be Heisenberg exchange with little contribution from static or diffusional dipolar effects. This is in keeping with conclusions from other work (24) and finds support from the data presented above. First, dipolar interactions from paramagnetic species in solution are small, as shown by the small Π values of NiAA and O_2 below the phase transition of DMPC (Fig. 4). Second, the Π values increase with increasing temperature, consistent with a mechanism dominated by Heisenberg exchange. Although the temperature dependence is complicated by changes in partition coefficient, this strengthens the conclusion for O_2 since its solubility decreases with temperature but Π increases.

Other methods have been reported for the determination of the immersion depth of a nitroxide spin label in bilayers. All are based on the magnitude of the dipolar interaction of the nitroxide with paramagnetic probes restricted to the aqueous phase. Likhtenstein *et al.* (5) describe a T_1 method in which the membrane is in a glassy matrix of 50% (vol/vol) glycerol containing uniformly distributed ferricyanide ions at 77 K. The decrease in T_1 of a nitroxide in the bilayer is shown to be proportional to the ferricyanide concentration and depends on the inverse third power of the distance from the surface. This distance dependence results from an integration of the nitroxide–metal ion static dipolar interaction over all aqueous ions. The dipolar effect is proportional to the product of the square of magnetic moment and T_2 of the metal center. This product was determined from the study of model systems, and the distance dependence was experimentally verified in the range of 7–22 Å.

Similarly, Innes and Brudvig (25) analyzed the dipolar-induced relaxation of a tyrosyl radical on the membrane-bound reaction center from *Rhodobacter sphaeroides* by Dy(III) uniformly distributed in a glassy matrix. The authors concluded that an inverse third power distance dependence from the membrane surface was required to fit the data.

Dalton *et al.* (4) investigated the dipolar interaction of Mn(II) and Gd(III) with *n*-doxyl PCs in bilayers at ambient temperature and interpreted the decrease in nitroxide signal intensity in terms of Leigh's theory (26) for the interaction of a single paramagnetic metal with a nitroxide, assuming that only the metal at the closest distance of approach was effective. The distance dependence was interpreted in terms of an inverse sixth power law. However, a reanalysis of their data indicates that it is better fit with an inverse third power distance dependence, suggesting that a mechanism involving nitroxide interaction with ions distributed in the aqueous phase may be more appropriate.

Recently, Pali *et al.* (6) reported that the integral saturation transfer EPR spectrum of *n*-doxyl PCs in dipalmitoyl PC bilayers in the gel phase at 0°C is sensitive to dipolar interactions with Ni(II) in solution. It was shown that the interaction depends on the inverse third power of the distance of the nitroxide from the bilayer surface.

All these methods depend on a spatial integration over the distribution of metal ions in solution. Since the ion distribution is uniform throughout the aqueous phase, this is straightforward for a simple electrically neutral bilayer containing spin-labeled phospholipids. On the other hand, the ion distribution in the aqueous phase is complex and unknown for bilayers containing charged lipids and proteins. In particular, if the distance of a nitroxide bound to a protein surface is desired, the problem may be serious since the aqueous domains of the protein will exclude an unknown volume of aqueous phase, and hence paramagnetic ions, at the closest distance of approach to the nitroxide. For the analysis of Likhtenstein *et al.* (5) and Innes and Brudvig (25), the systems were also in a frozen state at low temperature. The saturation transfer EPR method of Pali *et al.* (6) requires the bilayer to be in the solid state.

The method presented here overcomes these problems and should be applicable to complex membrane systems involving charged surfaces and proteins of unknown structure. A limitation of the collision gradient method presented here as applied to protein-bound nitroxides is that the nitroxide must be accessible to collision from the lipid phase.

In summary, the collision gradient method provides a strategy for the determination of immersion depth of a nitroxide from the bilayer surface. It is anticipated to be particularly useful for nitroxide side chains on transmembrane domains of proteins and requires no assumptions regarding the distributions of paramagnetic ions in the aqueous phase around the protein. The position of a transmembrane helix can in principle be determined from a single labeled mutant. Since low temperatures or solid phases are not required, the method may be used to monitor time-dependent helix translations that may accompany function, such as those recently proposed for the bacterial chemotactic aspartate receptor (27).

Research support was provided by National Institutes of Health Grants EY5216 (W.L.H.) and GM28289 and AI11479 (H.G.K.) and the Jules Stein Professor endowment (W.L.H.).

1. Altenbach, C., Marti, T., Khorana, H. G. & Hubbell, W. L. (1990) *Science* **248,** 1088–1092.
2. Greenhalgh, D. A., Altenbach, C., Hubbell, W. L. & Khorana, H. G. (1991) *Proc. Natl. Acad. Sci. USA* **88,** 8626–8630.
3. Shin, Y.-K., Levinthal, C., Levinthal, F. & Hubbell, W. L. (1993) *Science* **259,** 960–963.
4. Dalton, L. A., McIntyre, J. O. & Fleischer, S. (1987) *Biochemistry* **26,** 2117–2130.
5. Likhtenstein, G. I., Kulikov, A. V., Kotelnikov, A. I. & Levchenko, L. A. (1986) *J. Biochem. Biophys. Methods* **12,** 1–28.
6. Pali, T., Bartucci, R., Horváth, L. I. & Marsh, D. (1992) *Biophys. J.* **61,** 1595–1602.
7. Altenbach, C., Flitsch, S. L., Khorana, H. G. & Hubbell, W. L. (1989) *Biochemistry* **28,** 7806–7812.
8. Flitsch, S. L. & Khorana, H. G. (1989) *Biochemistry* **28,** 7800–7805.
9. Robinson, B. H., Mailer, C. & Haas, D. (1992) *Biophys. J.* **61,** A167.
10. Farahbakhsh, Z. F., Altenbach, C. & Hubbell, W. L. (1992) *Photochem. Photobiol.* **56,** 1019–1033.
11. Hubbell, W. L. & McConnell, H. M. (1971) *J. Am. Chem. Soc.* **93,** 314–326.
12. Brown, M. F., Seelig, J. & Häberlen, U. (1979) *J. Chem. Phys.* **70,** 5045–5053.
13. Griffith, O. H., Dehlinger, P. J. & Van, S. P. (1974) *J. Membr. Biol.* **15,** 159–192.
14. Shin, Y.-K. & Hubbell, W. L. (1992) *Biophys. J.* **61,** 1443–1453.
15. Hyde, J. S., Popp, C. A. & Schreier, S. (1978) *Front. Biol. Energ.* **2,** 1253–1261.
16. Henderson, R., Baldwin, J. M., Ceska, T. A., Zemlin, F., Beckmann, E. & Downing, K. H. (1990) *J. Mol. Biol.* **213,** 899–929.
17. Windrem, D. A. & Plachy, W. Z. (1980) *Biochim. Biophys. Acta* **600,** 655–665.
18. Subczynski, W. K. & Hyde, J. S. (1981) *Biochim. Biophys. Acta* **643,** 283–291.
19. Subczynski, W. K., Hyde, J. S. & Kusumi, A. (1989) *Proc. Natl. Acad. Sci. USA* **86,** 4474–4478.
20. Caffrey, M. & Feigenson, G. W. (1981) *Biochemistry* **20,** 1949–1961.
21. Vachon, A., Lecompte, C., Berleur, F., Roman, V., Fatome, M. & Braquet, P. (1987) *J. Chem. Soc. Faraday Trans. 1* **83,** 177–190.
22. Chattopadhyay, A. & London, E. (1987) *Biochemistry* **26,** 39–45.
23. Sillen, L. G. & Martell, A. E., eds. (1964) *Stability Constants of Metal-Ion Complexes, with Solubility Products of Inorganic Substances* (Chem. Soc., Burlington House, London) Spec. Publ. 17.
24. Hyde, J. S. & Sarna, T. (1978) *J. Chem. Phys.* **68,** 4439–4447.
25. Innes, J. B. & Brudvig, G. W. (1989) *Biochemistry* **28,** 1116–1125.
26. Leigh, J. S. (1970) *J. Chem. Phys.* **52,** 2608–2612.
27. Milligan, D. L. & Koshland, D. E., Jr. (1991) *Science* **254,** 1651–1654.